scientific reports

Check for updates

OPEN

Finite-element analysis of different fixation types after Enneking II + III pelvic tumor resection

Yu Sun[1,3], Haowen Xue[1,3], Xiaonan Wang[1], Jiaxin Zhang[1], Zezhou Xu[2], Yunting Guo[2], Renlong Xin[2], Zhenglei Yu[2], Qing Han[1], Xin Zhao[1]✉, Jincheng Wang[1]✉ & Luquan Ren[2]✉

The current primary treatment approach for malignant pelvic tumors involves hemipelvic prosthesis reconstruction following tumor resection. In cases of Enneking type II + III pelvic tumors, the prosthesis necessitates fixation to the remaining iliac bone. Prevailing methods for prosthesis fixation include the saddle prosthesis, ice cream prosthesis, modular hemipelvic prosthesis, and personalized prosthetics using three-dimensional printing. To prevent failure of hemipelvic arthroplasty protheses, a novel fixation method was designed and finite element analysis was conducted. In clinical cases, the third and fourth sacral screws broke, a phenomenon also observed in the results of finite element analysis. Based on the original surgical model, designs were created for auxiliary dorsal iliac, auxiliary iliac bottom, auxiliary sacral screw, and auxiliary pubic ramus fixation. A nonlinear quasi-static finite element analysis was then performed under the maximum load of the gait cycle, and the results indicated that assisted sacral dorsal fixation significantly reduces stress on the sacral screws and relative micromotion exceeding 28 μm. The fixation of the pubic ramus further increased the initial stability of the prosthesis and its interface osseointegration ability. Therefore, for hemipelvic prostheses, incorporating pubic ramus support and iliac back fixation is advisable, as it provides new options for the application of hemipelvic tumor prostheses.

Keywords Malignant, Pelvic tumor, Prosthesis, Finite element analysis

Pelvic tumors are ranked as the third most prevalent form of malignant bone tumors, constituting approximately 5–15% of all malignant bone tumors, and exhibit high malignancy, rapid disease course, and poor prognosis[1]. The current primary treatment approach for malignant pelvic tumors involves hemipelvic prosthesis reconstruction following tumor resection. In cases of Enneking type II + III pelvic tumors, the prosthesis necessitates fixation to the remaining iliac bone. Prevailing methods for prosthesis fixation include the saddle prosthesis, ice cream prosthesis, modular hemipelvic prosthesis, and personalized prosthetics using three-dimensional (3D) printing[2–8].

Hemipelvic prostheses have demonstrated varied clinical outcomes. Both modular and individualized hemipelvic prostheses have been substantiated to offer enhanced initial stability and postoperative functionality. Both types of prostheses can provide mechanical fixation using iliac plates and screws. Mechanical failures of prostheses, such as periprosthetic fractures and screw breakage, can lead to the deterioration of the remaining iliac bone, increase the complexity of surgical revisions, and escalate the economic and psychological burdens on patients[8]. Therefore, establishing robust prosthesis fixation is pivotal in achieving success in hemipelvic replacements.

Presently, the hemipelvic prosthesis is primarily fixed to the iliac bone through iliac screws. These screws are subjected to the shear stress transmitted across the trunk and lower limbs. Excessive shear stress can lead to screw breakage, which is a critical factor contributing to prosthesis failure. Consequently, minimizing stress on the iliac screws and enhancing prosthesis stability are pivotal objectives in hemipelvic prosthesis design[9]. Conversely, individualized customized prostheses offer the advantage of perfect alignment with the patient anatomy based on surgical planning[10,11]. However, the diverse structures of individualized customized prostheses raise uncertainties regarding the optimal structural design necessary to ensure stable biomechanical properties for patients.

We, therefore, aimed to investigate the stability of hemipelvic prostheses using a combination of case report and finite element analysis. The original structure of the hemipelvic prosthesis serves as the foundation to explore stress and microstructure dynamics, and incorporates enhancements like an iliac back plate, sacral screws, and an iliac platform to evaluate the impact thereof. Additionally, we examined the influence of an anatomically

[1]Orthopaedic Hospital, The Second Hospital of Jilin University, Changchun 130012, China. [2]Key Laboratory of Engineering Bionics, Ministry of Education, Jilin University, Changchun 130012, China. [3]These authors contributed equally: Yu Sun and Haowen Xue. ✉email: xzhao@jlu.edu.cn; wangjinc@jlu.edu.cn; lqren@jlu.edu.cn

designed pelvic ring, realized by incorporating a pubic ramus design, on the overall stability of the hemipelvic prosthesis. This approach is essential to ascertain the initial stability of the prosthesis.

Materials and methods

Case report

A retrospective analysis was conducted on a patient who underwent hemipelvic replacement at the Second Hospital of Jilin University, Changchun, China. The patient was a 73-year-old female who underwent left hemipelvic resection and artificial hemipelvic replacement due to left hip pain accompanied by restricted mobility. PET-CT results showed that left acetabular, pubic and ischial bones destruction and soft tissue mass, invading the lower part of the left femoral head neck, with increased metabolism, suggesting malignant tumor. Pathological results showed that thyroid follicular tissue was suspected to be metastatic thyroid follicular carcinoma. Immunohistochemical staining results showed CK (AE1/AE3) (+), ER (−), PR (−), Ki67 (positive rate 10%), PAX-8 (+), TTF-1 (+), TG (+), GATA3 (−). CT and MRI fusion images could be found in Supplementary material 1. And, this patient underwent thyroid lesion resection surgery four months ago. Six months after the operation, patient complained that there was no obvious cause leading to hip pain and a pelvic radiograph revealed loosening of the prosthesis and a broken screw (Fig. 1). During this period, the patient underwent thyroid tumor chemotherapy treatment. This study received approval from the Ethics Committee of the Second Hospital of Jilin University (SB [2021] No. 152). This participant was informed and signed informed consent forms.

3D reconstruction of surgical model

Based on the preoperative design and postoperative thin-Sect. (0.625 mm) computed tomography (CT) scan imaging data, the patient's pelvis and prosthetic structure were segmented using Mimics 19.0 software (Materialize, Belgium), and the model was subsequently imported into SolidWorks software (Dassault Systèmes) in STL format. Following this, the shape and contour of the hemipelvic prosthesis were refined, and the preliminary model was exported to Magics 19.0 software (Materialise Company, Belgium) for size adjustment, surface smoothing, and other modifications. Based on the observed operative conditions, four 6.5 mm diameter iliac locking screws (25 mm, 55 mm, 55 mm, and 50 mm) were surgically implanted. The integration of a 3D reconstruction model with postoperative imaging clearly demonstrates that the prosthetic reconstruction aligns well with the intended design (Fig. 1). The prosthesis was 3D printed and simulated for surgery, and bone-contact surface of the implant was designed with porous-coated (Supplementary material 2). Due to the controversy surrounding the fixation of the pubic, the connection of pubic and was not selected (Fig. 1).

Design and simulation of pelvic prosthesis

Originating from the original hemipelvic prosthesis (A), and utilizing the auxiliary fixation provided by the available space around the ilium, including the iliac posterior aspect, the bottom, and the sacral side, a novel prosthesis fixation method was designed as follows: (B) fixation was introduced through an iliac fixation plate positioned behind the ilium tried to increase the contact area behind the prosthesis and limit its introversion; (C) the contact area of the iliac platform at the bottom was expanded and tried to increase the contact area beneath the prosthesis and limit its internal rotation; and (D) sacral fixation strength was enhanced with additional sacral screws in order to restrict the movement of prosthesis. Fixation methods demonstrating optimal initial stability for the prosthesis were selected, and the mechanical characteristics of the pubic ramus support-assisted fixation were verified, which were designed on the basis of original hemipelvic prosthesis (A) and the addition of iliac back fixation (B), with a 60 mm pubic ramus locking screw and a 50 mm ischial ramus locking screw (Figs. 2, 5).

We then imported the designed model into Hypermesh 2020 software (Altair) using the STL file format and performed two-dimensional (2D) mesh partitioning. Through grid quality sensitivity analysis, we determined a triangular mesh size of 1 mm. Subsequently, we converted the 2D mesh to solid, using C3D4 tetrahedral elements as the unit format.

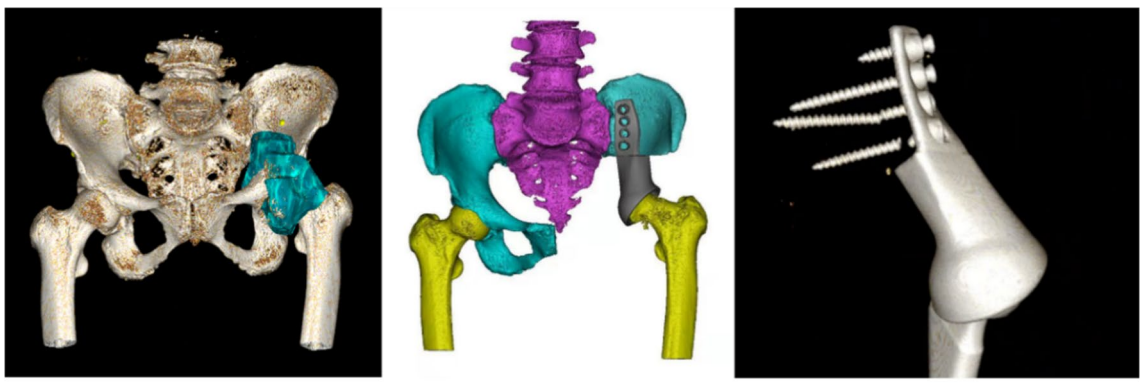

Fig. 1. Three-dimensional (3D) reconstruction model diagram. (**a**) Preoperative 3D reconstruction (Green: the region of tumor), (**b**) preoperative design, (**c**) postoperative 3D reconstruction with broken screw.

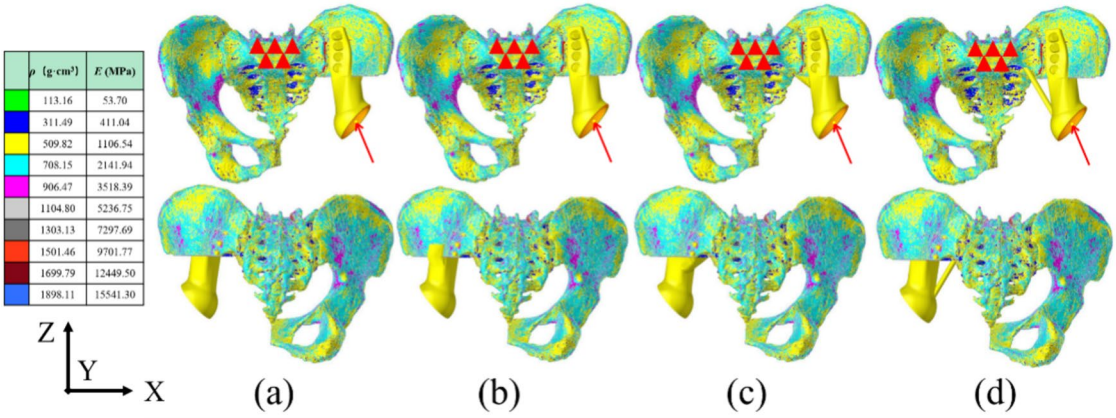

Fig. 2. Pelvis finite element analysis model. (**a**) original hemipelvic model, (**b**) assisted posterior iliac fixation, (**c**) assisted bottom iliac fixation, (**d**) assisted sacral screw fixation. Triangle: Constraints, Arrow: Force.

The bone model utilized heterogeneous material assignment, based on varying bone CT grayscale values (in Hounsfield units, Hu), according to the following formula (Fig. 2)[12]:

$$\rho(\mathrm{Kg/m^3}) = 47 + 1.122\ \mathrm{Hu} \tag{1}$$

$$E(\mathrm{MPa}) = 0.63\rho^{1.35} \tag{2}$$

$$\mu = 0.3$$

The elastic modulus for the sacroiliac joint and pubic symphysis was set to 15 MPa, with a Poisson's ratio of 0.45. The hemipelvic prosthesis, made of titanium alloy (Ti6Al4V), has an elastic modulus of 110 GPa and a Poisson's ratio of 0.30[8].

The upper edge of the Sacral 1 vertebra was set as a constraint, with the degrees of freedom for each node set to 0. Both the sacroiliac joint and pubic symphysis were defined as tied contacts. Frictional contact between the prosthesis and bone was established, with a coefficient of friction of 0.88 ($\mu = 0.88$) for the screw-bone interface and 0.30 ($\mu = 0.30$) for the prosthesis-bone interface[8]. Load conditions, based on gait analysis data for the pelvis by Bergmann et al., were uniformly applied at the acetabulum. The applied load was calculated as 1,948 N, based on the patient's weight and load ratio, and was then applied to the model[13]. Joint and muscle forces were fitted through internal sensors in the hip joint by the research team; therefore, the finite element analysis model in this study does not include separately modeled muscles and ligaments around the hip joint (Fig. 2). The OptiStruct solver (Altair) was used and the unit information was showed on Table 1.

All methods were performed in accordance with the relevant guidelines and regulations.

Results

The results from the stress distribution analysis show that stress is primarily concentrated at the interface between the prosthesis and the sacroiliac region on the affected side, without significant stress transmission to the healthy pelvis side. After the addition of iliac back fixation (B), bottom fixation (C), and sacral screw reinforced fixation (D), there was a noticeable reduction in stress on the prosthesis side, along with increased stress concentration on the auxiliary fixation areas. Notably, the inclusion of sacral screw auxiliary fixation resulted in a more significant adjustment in stress distribution, whereas the impact of adding bottom fixation (C) was relatively minor (Fig. 3).

A stress analysis of the prosthesis revealed that stress was primarily concentrated at the tips of the third and fourth iliac screws, with a maximum stress value of 295.7 MPa. Despite the addition of iliac back fixation (B) and bottom fixation (C), stress distribution remained focused at the screw connections, with maximum stresses

Component	Prosthesis	Ilium	Sacrum	Healthy side pelvis
A	248,619	542,751	754,352	644,200
B	257,144	542,751	754,352	644,200
C	267,244	542,751	754,352	644,200
D	267,947	542,751	763,903	644,200
A*	398,555	542,751	763,903	726,910
B*	408,610	542,751	763,903	726,910

Table 1. Number of elements in finite element analysis components.

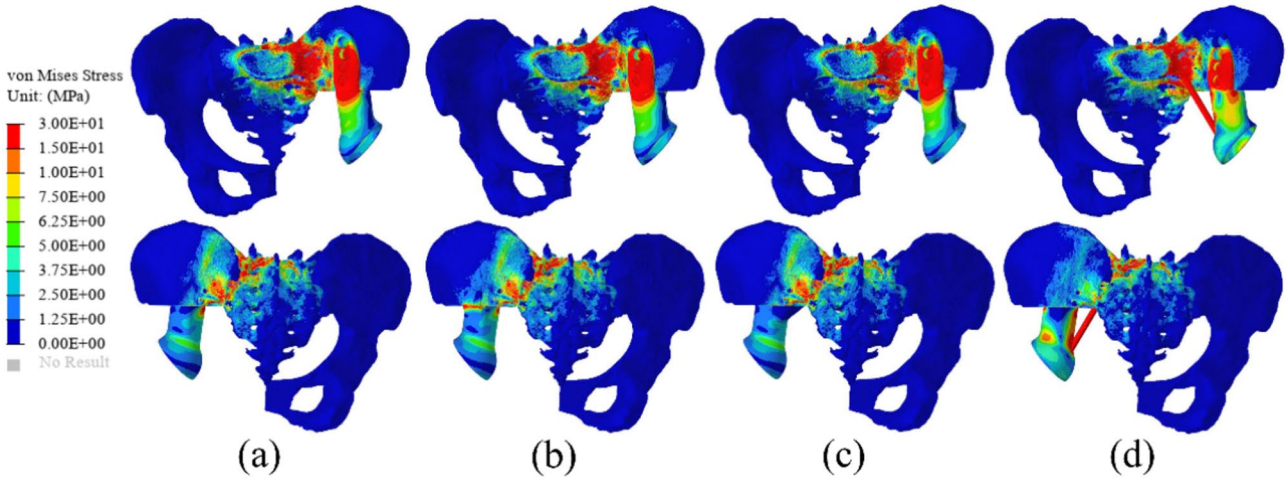

Fig. 3. The stress distribution of the pelvis. (**a**) Original hemipelvic model, (**b**) assisted posterior iliac fixation, (**c**) assisted bottom iliac fixation, (**d**) assisted sacral screw fixation.

of 235.3 MPa and 265.1 MPa, respectively. After the introduction of sacral screw fixation (D), stress concentration shifted to the sacral screws, peaking at 572.8 MPa, whereas the stress at the connection of the fourth screw reduced to 184.5 MPa (Fig. 4).

Based on the above results, the addition of iliac back fixation (B) was selected as the optimal initial stability for the prosthesis, then the pubic ramus support-assisted fixation was supplemented (B*), and compared with the original prosthesis with the pubic ramus support-assisted fixation (A*). Following the addition of pubic fixation, the stress analysis indicated that stress was primarily distributed across the prosthesis, both sacroiliac joints, and the pelvic bone on the healthy side, resulting in a ring-shaped stress distribution. Stress distribution on the prosthesis was concentrated at the pubic symphysis screw connections, exhibiting maximum stresses of 264.5 MPa. The stress at the connection of the fourth iliac screw decreased to 218.8 MPa. Upon adding fixation to the iliac back, the stress at the pubic symphysis screw connection reduced to 226.7 MPa, and at the connection of the fourth iliac screw decreased to 209.7 MPa (Fig. 5).

Five measurement zones were selected on each side of the pelvic ring structure, where average stresses were measured. Subsequently, the average stresses of the entire pelvic ring structure were calculated. Radar chart results show that, without pubic support, stress concentration occurs in the L2 region. Following the addition of pubic fixation, the stress distribution becomes more uniform. Average stress results for the pelvic ring

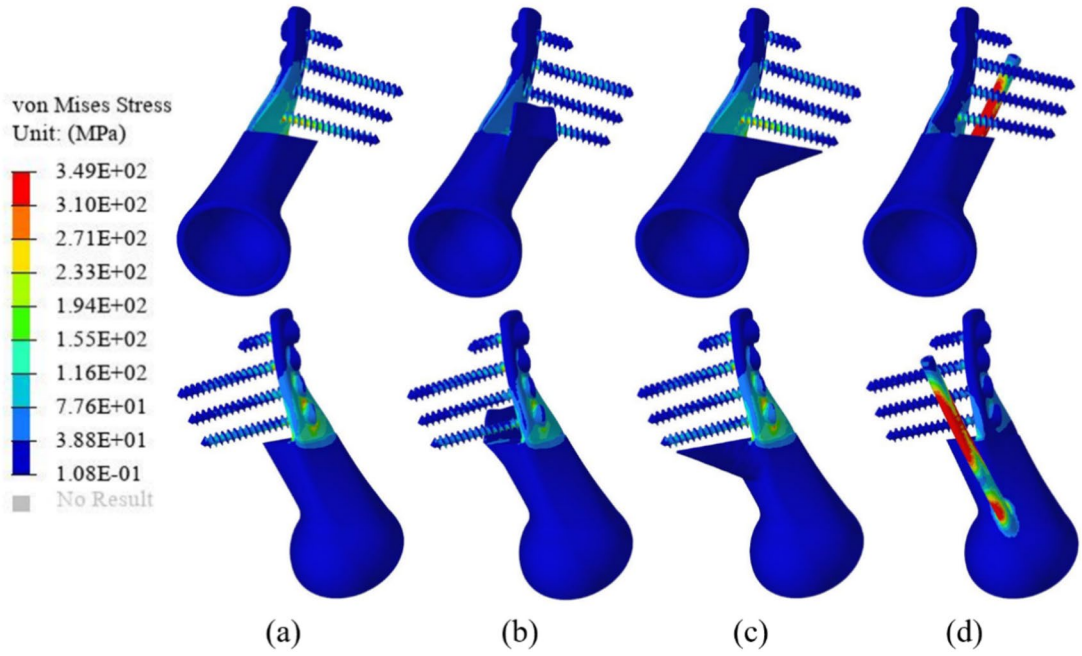

Fig. 4. The stress distribution of the prosthesis. (a) Original hemipelvic model, (**b**) assisted posterior iliac fixation, (**c**) assisted bottom iliac fixation, (**d**) assisted sacral screw fixation.

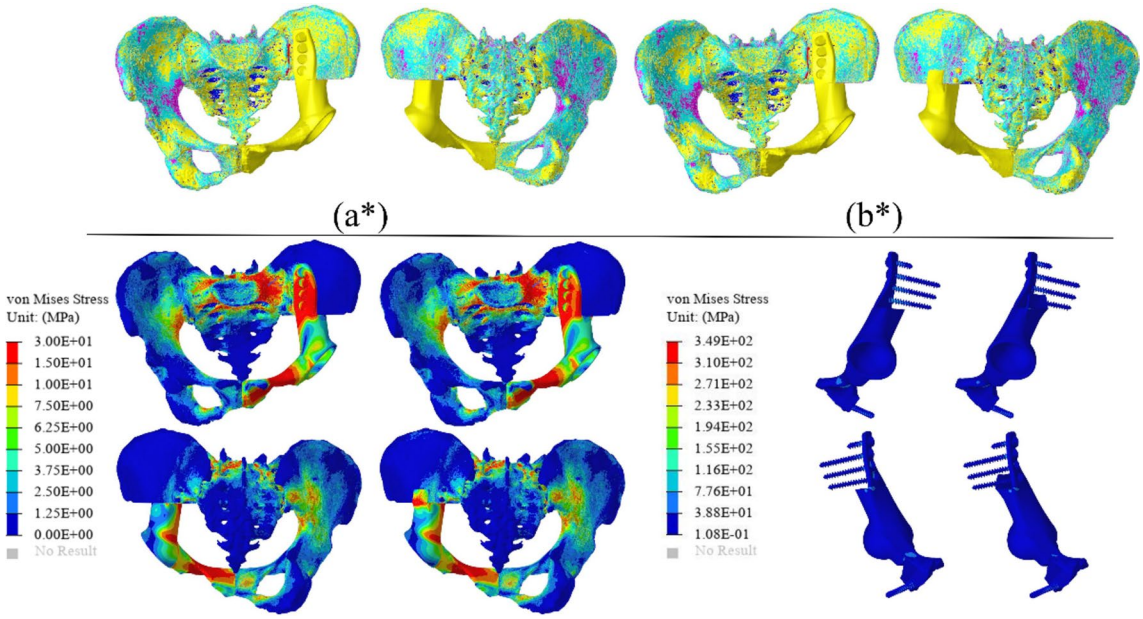

Fig. 5. The stress distribution of assisted pubic fixation. (**a***) Original hemipelvic model assisted pubic fixation, (**b***) assisted posterior iliac and pubic fixation.

demonstrated significant differences within groups lacking pubic ramus support. Upon adding pubic ramus support, the standard deviation within groups decreased, and the introduction of additional iliac back fixation significantly increased the overall average stress ($p < 0.05$) (Fig. 6).

Micromotion analysis revealed that areas exceeding 28 μm were predominantly concentrated on the inner side of the iliac plate. Adding auxiliary fixation consistently reduced the area on the iliac plate exceeding 28 μm. Specifically, enhancing fixation at the back, bottom, and sacral screw areas can improve the integration capacity of the interface bone by increasing the contact area. With the introduction of pubic ramus support, a further reduction in the micromotion area of the iliac plate was observed (Fig. 7).

Discussion

The pelvis and its surrounding soft tissues represent a common site for tumors[1]. Due to the subtlety of early symptoms, pelvic malignant tumors are often in advanced stages when discovered, characterized by large size and indistinct boundaries with surrounding tissues. Advancements in comprehensive treatment and surgical techniques have led to the predominance of limb-salvage treatments for pelvic tumors. In cases of pelvic tumors in zones II + III, the integrity of the pelvic ring is compromised, posing challenges in reconstructing pelvic structure and function. Currently, the options for pelvic tumor prostheses in zones II + III are limited, primarily including saddle-type, ice cream, and customized prostheses[2,4,14]. However, the use of saddle-type and ice cream prostheses has declined due to high rates of infection and loosening, and the requirement for substantial support in saddle-type prostheses. With advancements in 3D printing technology, clinically applied hemipelvic prostheses are increasingly being fabricated using 3D printing.

Currently, the design process for 3D printed hemipelvic prostheses involves preoperative design, prosthesis verification, surgical planning, and other preparations before clinical application[8,15]. Prosthesis refinement requires referencing physical and chemical performance tests, as well as clinical follow-up results, to gradually

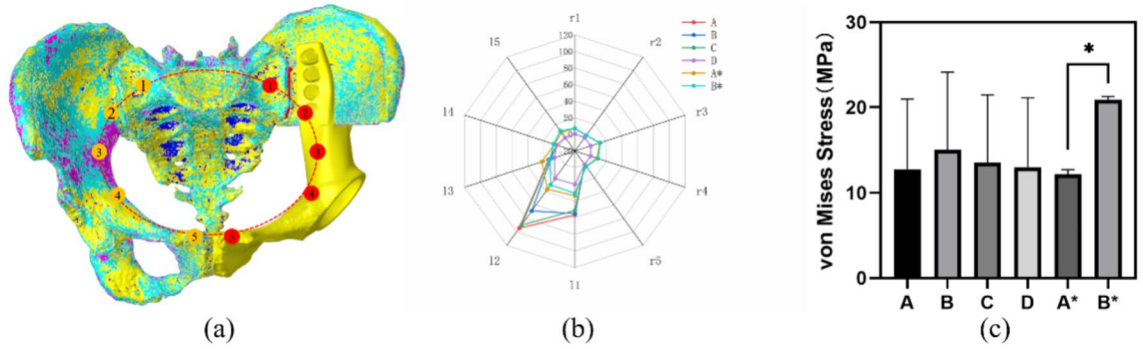

Fig. 6. Pelvic circular stress distribution test. (**a**) The mark point of stress distribution, (**b**) radar chart of stress distribution at landmark points, (**c**) statistical chart of stress at landmark points.

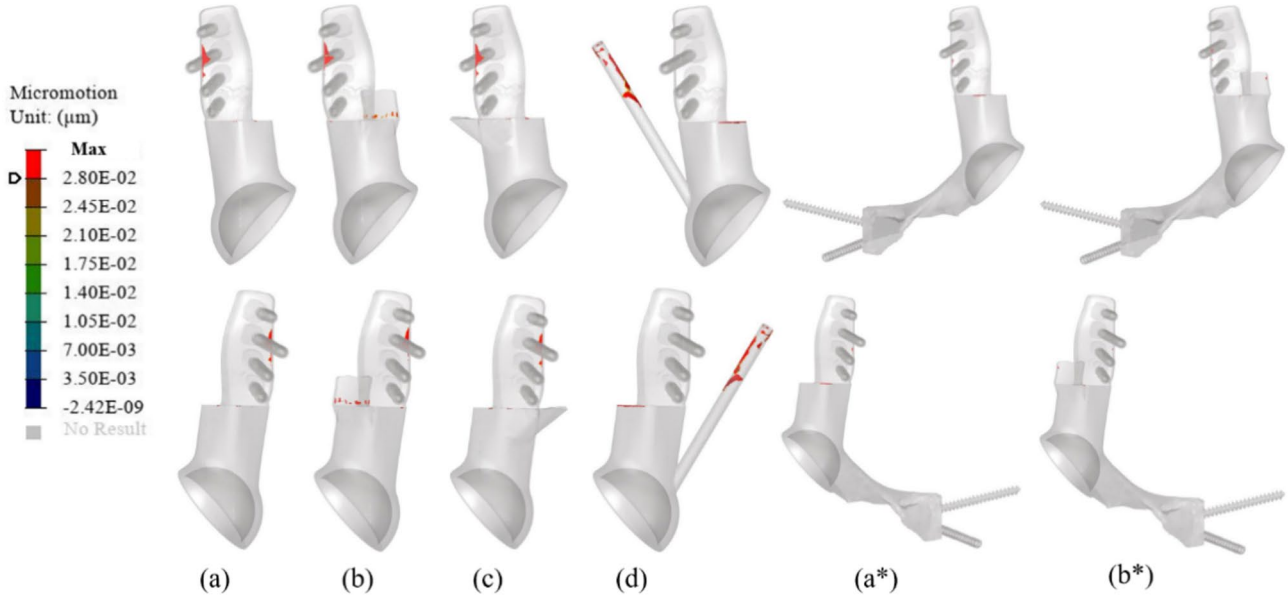

Fig. 7. The distribution of relative micromotion. Red: Relative micromotion exceeding 28 μm.

improve the design, thereby enhancing the initial stability of the hemipelvic prosthesis. This study was prompted by the discovery of broken iliac screws in a patient after hemipelvic replacement in zones II + III (Fig. 1). To analyze the causes of screw breakage and offer a theoretical basis to design future hemipelvic prostheses, this study examined the stress and micromotion post-initial implantation and sought to enhance the prosthesis design.

Stress serves as a crucial indicator to evaluate the initial stability and the risk of screw breakage following prosthesis implantation. Results from the postoperative reconstruction model reveal stress concentration at the tips of the third and fourth iliac screws, with a maximum stress of 295.7 MPa, which approaches the fatigue limit of Ti6Al4V (300–310 MPa)[16]. This finding indicates a potential risk of screw breakage, effectively validating actual clinical occurrences. The addition of auxiliary fixation results in a noticeable reduction in screw stress, with sacral screw fixation showing the most significant decrease (37.6%). However, the high stress concentration at the sacral screw (572.8 MPa) raises concerns and potential clinical apprehensions. In comparison, the addition of iliac back fixation also significantly reduces screw stress (20.4%), with the maximum stress on the prosthesis suggesting relative safety (235.3 MPa). Therefore, among the evaluated auxiliary fixation methods, iliac back fixation is recommended as a safer option (Figs. 3 and 4).

Many clinically used modular hemipelvic prostheses currently lack a pubic ramus design[10,11]. Although customized 3D-printed hemipelvic prostheses often include pubic ramus fixation, the necessity of adding a pubic ramus design remains debated[17,18]. The rigid connection of components after adding pubic ramus support might lead to excessive tension, and such a connection between the pubic ramus support and the bone/acetabulum may lack sufficient strength[10]. Nevertheless, the absence of pubic ramus support may lead to an incomplete pelvic ring, disrupting normal biomechanical transmission and potentially causing mechanical failure of the prosthesis[19,20]. Thus, investigating the biomechanical mechanisms of pubic ramus support-assisted fixation and addressing concerns like excessive tension in the pubic ramus support holds significant scientific importance to resolve current clinical debates. Stress results indicate that the addition of pubic ramus support restores the mechanical transmission circular structure of the pelvis. Stress distribution significantly increases on the healthy side of the pelvis, achieving a more uniform overall stress distribution. The maximum stress on the prosthesis shifts to the pubic symphysis screw connection (264.5 MPa), ensuring a stable reconstruction of the prosthesis. Furthermore, adding iliac back fixation to the pubic ramus support foundation results in a decrease of the maximum stress at the iliac screw to 209.7 MPa, and at the pubic symphysis screw to 226.7 MPa. This represents a 29.1% decrease in maximum stress at the iliac screw compared to intraoperative conditions. Additionally, the significant increase in average stress on the pelvic ring ($p < 0.05$) indicates a more uniform stress distribution within the pelvic ring structure, further enhancing the initial stability of the prosthesis (Figs. 5 and 6).

Micromotion serves as a crucial indicator in assessing the bone-implant interface integration capability. Micromotions of less than 28 μm at the contact interface promote bone integration, whereas micromotions between 30 and 150 μm result in the formation of both bone and fibrous tissue. Micromotions exceeding 150 μm predominantly result in fibrous tissue formation[21]. The long-term stability of the prosthesis depends on its initial stability, underscoring the importance of minimizing micromotion at the interface. Results show that the addition of auxiliary fixation consistently reduces the area of the iliac plate exceeding 28 μm. Furthermore, implementing micro-hole designs at the interface through auxiliary fixation further enhances bone integration capability. These fixation methods enhance prosthesis stability by increasing the area available for bone integration, thereby laying the foundation for the long-term biological fixation of pelvic prostheses. Among these methods, auxiliary sacral back fixation demonstrates optimal potential for interface bone integration, with pubic ramus support further enhancing the bone integration potential of the prosthesis (Fig. 7).

This study has certain limitations, including the absence of in vitro biomechanical experiments. Future studies may aim to construct a biomechanical model and supplement it with mechanical experiments. We utilized peak loads from gait cycles without simulating variations in the pelvic prosthesis throughout the gait cycle. The analysis was limited to several common fixation methods for hemipelvic prostheses currently used in clinical practice. In addition, adding longitudinal screws to the iliac bone, expanding the range of prosthetic iliac plates and changing the direction of the iliac screw also could be tried to reduce stress on the implant and improve longevity. Future research should include additional fixation methods to build a comprehensive evaluation system for hemipelvic prostheses.

In summary, to address the challenge of inadequate initial stability in pelvic tumor fixation in Enneking II + III, adding iliac back, bottom, and sacral screw fixation to the original prosthesis can significantly reduce the maximum stress on the iliac screws. Considering overall stress, iliac back fixation results in relatively lower stress and effectively reduces iliac screw stress. Furthermore, supplementary pubic ramus support can further decrease screw stress, reduce the micromotion area exceeding 28 μm, and restore the circular stress structure of the pelvic ring, thus enhancing the prosthesis initial stability. Therefore, it is advisable for hemipelvic prostheses to include pubic ramus support and iliac back fixation, offering new options for the application of hemipelvic tumor prostheses.

Data availability

All data generated or analysed during this study are included in this published article.

Received: 9 April 2024; Accepted: 27 August 2024
Published online: 06 September 2024

References

1. Jansen, J. A., van de Sande, M. A. J. & Dijkstra, P. D. S. Poor long-term clinical results of saddle prosthesis after resection of periacetabular tumors. *Clin. Orthop. Relat. Res.* **471**(1), 324–331 (2013).
2. van der Lei, B. *et al.* The use of the saddle prosthesis for reconstruction of the hip joint after tumor resection of the pelvis. *J. Surg. Oncol.* **50**(4), 216–219 (1992).
3. Danışman, M. *et al.* Reconstruction of periacetabular tumours with saddle prosthesis or custom-made prosthesis, functional results and complications. *Hip. Int.* **26**(2), e14–e18 (2016).
4. Issa, S. P. *et al.* Pelvic reconstructions following peri-acetabular bone tumour resections using a cementless ice-cream cone prosthesis with dual mobility cup. *Int. Orthop.* **42**(8), 1987–1997 (2018).
5. Wong, K. C. 3D-printed patient-specific applications in orthopedics. *Orthop. Res. Rev.* **8**, 57–66 (2016).
6. Xu, S. *et al.* Reconstruction of tumor-induced pelvic defects with customized. Three dimensional printed prostheses. *Front. Oncol.* **12**, 935059 (2022).
7. Ji, T. *et al.* 3D-printed modular hemipelvic endoprosthetic reconstruction following periacetabular tumor resection: Early results of 80 consecutive cases. *J. Bone Joint Surg. Am.* **102**(17), 1530–1541 (2020).
8. Zhao, X. *et al.* Novel 3D printed modular hemipelvic prosthesis for successful hemipelvic arthroplasty: A case study. *J. Bionic Eng.* **15**(6), 1067–1074 (2018).
9. Ji, T. and W. Guo, Reconstruction after ilium resection. In *Surgery of the pelvic and sacral tumor*. 2020. p. 77–80.
10. Ji, T. *et al.* Modular hemipelvic endoprosthesis reconstruction–experience in 100 patients with mid-term follow-up results. *Eur. J. Surg. Oncol.* **39**(1), 53–60 (2013).
11. Ji, T. *et al.* Reconstruction of type II+III pelvic resection with a modular hemipelvic endoprosthesis: A finite element analysis study. *Orthop. Surg.* **2**(4), 272–277 (2010).
12. Rho, J. Y., Hobatho, M. C. & Ashman, R. B. Relations of mechanical properties to density and CT numbers in human bone. *Med. Eng. Phys.* **17**(5), 347–355 (1995).
13. Bergmann, G. *et al.* Hip contact forces and gait patterns from routine activities. *J. Biomech.* **34**(7), 859–871 (2001).
14. Guo, W. *et al.* Reconstruction with modular hemipelvic prostheses for periacetabular tumor. *Clin. Orthop. Relat. Res.* **461**, 180–188 (2007).
15. Zhou, Y. *et al.* Finite element analysis of the pelvis after modular hemipelvic endoprosthesis reconstruction. *Int. Orthop.* **37**(4), 653–658 (2013).
16. Long, M. & Rack, H. J. Titanium alloys in total joint replacement—a materials science perspective. *Biomaterials* **19**(18), 1621–1639 (1998).
17. Li, Z. *et al.* Treatment of pelvic giant cell tumor by wide resection with patient-specific bone-cutting guide and reconstruction with 3D-printed personalized implant. *J. Orthop. Surg. Res.* **18**(1), 648 (2023).
18. Hu, X. *et al.* Combined and modified gibson and ilioinguinal approaches in Type II + III Internal hemipelvectomy for periacetabular tumors. *Front. Oncol.* **12**, 934812 (2022).
19. Liu, D. *et al.* Design and biomechanical study of a novel adjustable hemipelvic prosthesis. *Med. Eng. Phys.* **38**(12), 1416–1425 (2016).
20. Liu, D. *et al.* Biomechanical analysis of a novel hemipelvic endoprosthesis during ascending and descending stairs. *Proc Inst Mech Eng H* **230**(10), 962–975 (2016).
21. Pilliar, R. M., Lee, J. M. & Maniatopoulos, C. Observations on the effect of movement on bone ingrowth into porous-surfaced implants. *Clin. Orthop. Relat. Res.* **208**, 108–113 (1986).

Acknowledgements

National Natural Science Foundation of China (82272504, 82072456, 52375289, 52205310); Wu Jieping Medical Fund (320.6750.18522) Jilin Provincial Department of Science and Technology (20220402067GH, 202201ZYTS129, YDZJ202201ZYTS046); Jilin Provincial Development and Reform Commission (2022C044-2); Changchun Science and Technology Bureau Outstanding Youth Fund (ZKICKJJ2023015); Jilin University Outstanding Youth Cultivation Project (419070623036), Innovative research and development team for bone implants based on additive manufacturing of Jilin University (419070623054); The batch of grant from China Postdoctoral Science Foundation (2023M741341); The Batch of Special Grants from China Postdoctoral Science Foundation (2023TQ0129); The Natural Science Foundation of Shandong Province (ZR2021QE263).

Author contributions

JW and XZ were contributor to the conceptualization. LR was contributor to contributed to review and editing. YS and HX were contributor to software, and writing—original draft; XW, JZ and RX were contributor to software and writing—review. Funding acquisition contributed by XZ, JW,QH, ZX, ZY and YG. All authors have read and agreed to the published version of the manuscript.

Competing interests

The authors declare no competing interests.

Ethical approval

This study was approved by the Ethics Committee of the Second Hospital of Jilin University (No. 152 in 2021).

Additional information

Supplementary Information The online version contains supplementary material available at https://doi.org/10.1038/s41598-024-71334-1.

Correspondence and requests for materials should be addressed to X.Z., J.W. or L.R.

Reprints and permissions information is available at www.nature.com/reprints.

Publisher's note Springer Nature remains neutral with regard to jurisdictional claims in published maps and institutional affiliations.